Journal of Ceramic Processing Research. Vol. 22, No. 3, pp. 296~300 (2021)
(Received 18 June 2020, Received in revised form 11 December 2020, Accepted 29 December 2020)
https://doi.org/10.36410/jcpr.2021.22.3.296

J O U R N A L O F
Ceramic Processing Research

Microwave sintering and mechanical properties of La_2O_3/Nb_2O_5 toughened Al_2O_3 ceramics

Jin Liu, Bingliang Liang*, Yunlong Ai, Jianjun Zhang, Fei He, Wen He and Zhiyong Liu
School of Materials Science and Engineering, Nanchang Hangkong University, No.696, South Fenghe Avenue, Nanchang 330063, Jiangxi Province, P.R. China

To improve the toughness of Al_2O_3 ceramic, $xLa_2O_3/10Nb_2O_5$-$(90–x)Al_2O_3$ (x = 2.5-15.0 vol.%) composite ceramics were synthesized via microwave-sintering. The influences of sintering temperature (T_s) and La_2O_3 content on phase composition and mechanical property of $xLa_2O_3/10Nb_2O_5$-$(90–x)Al_2O_3$ composite ceramics were studied. It is shown in the results that the T_s of La_2O_3/Nb_2O_5 doped Al_2O_3 ceramic was 150 ºC lower than that of Al_2O_3 ceramic. With the increase of x, $La_{0.33}NbO_3$, $LaNbO_4$ and $LaAl_{11}O_{18}$ were formed successively. $LaNbO_4$, columnar-Al_2O_3 grains and $LaAl_{11}O_{18}$ with plate-like shape were generated in-situ during the sintering period. Compared to Al_2O_3 ceramic, the fracture toughness of $xLa_2O_3/10Nb_2O_5$-$(90–x)Al_2O_3$ ceramics were at least 70% higher when $5.0 \le x \le 12.5$. $7.5La_2O_3/10Nb_2O_5$-$82.5Al_2O_3$ ceramic exhibited superior mechanical property: Hv = 12.0 GPa, K_{IC} = 6.2 MPa·m$^{1/2}$ (1,500 ºC, 30 min).

Keywords: Al_2O_3 ceramics; Microwave sintering; Phase formation; Mechanical properties

Introduction

Alumina (Al_2O_3) ceramic ranks among the most important engineering ceramics due to high hardness, high mechanical strength, high temperature insulation resistance, excellent thermal conductivity [1]. However, its potential application in engine is limited by high fragility (K_{IC}-3.0 MPa·m$^{1/2}$) [2]. Some additives or second phases such as $AlCr_2$ [3], WC [4], TiC [5, 6], SiC [7, 8], ZrO_2 [9, 10], Nb_2O_5 [11, 12], La_2O_3 [13], $LaAl_{11}O_{18}$ [14], $LaNbO_4$ [15] were doped into the Al_2O_3 matrix to improve mechanical properties. In Al_2O_3-Nb_2O_5 [12] system, some equiaxed Al_2O_3 grains were induced to grow oriented into columnar grains. As to Al_2O_3-La_2O_3 [13] and Al_2O_3-$LaAl_{11}O_{18}$ [14] systems, the plate-like $LaAl_{11}O_{18}$ grains significantly improved the fracture toughness of Al_2O_3. Furthermore, the fracture toughness and bending strength of Al_2O_3 was improved by the domain conversion of $LaNbO_4$ [15, 16].

Generally, ceramics can be sintered by conventional, plasma and microwave heating methods [17-19]. Microwave sintering, as an efficient sintering method, leads to the volume heating of the sample through the coupling between microwave radiation and the material [20, 21]. Therefore, the temperature gradients resulted from conventional sintering process is prevented [22, 23]. In this experiment, in order to form $LaNbO_4$ and plate like $LaAl_{11}O_{18}$ grains in-situ and improve the mechanical property, Al_2O_3 were doped with La_2O_3/Nb_2O_5 ($xLa_2O_3/10Nb_2O_5$-$(90–x)Al_2O_3$, x = 2.5-15.0 vol.%) and synthesized via microwave-sintering.

*Corresponding author:
Tel : +86 791 8386 3034
Fax: +86 791 8645 3203
E-mail: lbl@nchu.edu.cn

Experimental Procedure

$xLa_2O_3/10Nb_2O_5$-$(90–x)Al_2O_3$ (x = 2.5-15.0 vol.%) composite ceramics were synthesized via microwave-sintering. High purity La_2O_3 (99.99 wt.%), Nb_2O_5 (99.99 wt.%) and Al_2O_3 (99.6 wt.%) were weighed according to the volume ratio of $xLa_2O_3/10Nb_2O_5$-$(90–x)Al_2O_3$ and then ball milled for 12 h. After dried, the mixed powders were granulated with 5 wt.% polyvinyl alcohol solution (PVA, 10 wt.%) as binder. Then granulated mixtures were pressed into regular bars by uniaxial (100 MPa) and cold-isostatic pressing (200 MPa) successively. These regular bars were placed in a conventional furnace and calcined at 600 ºC for 3 h to remove binder. The sintering temperature of the samples in the microwave sintering furnace was 1,450~1,500 ºC and the holding time was 30 min.

All sintered specimens were polished before the test. Their densities were evaluated by the Archimedes method. The phase analysis was carried out by X-ray diffractometry (XRD, D8ADVANCE Diffractometer, Bruker-AXS). The observation of microstructure were performed on thermal etched specimens by scanning electron microscopy (SEM, Nova Nano SEM450, FEI). The elemental analysis was conducted using energy dispersed spectroscopy (EDS). Vickers hardness (Hv) and fracture toughness (K_{IC}) was tested by HVS-1000

Vickers tester and single edge precracked beam method (SEPB), respectively.

Results and Discussion

The relative density (h) of $x La_2O_3/10Nb_2O_5$-$(90–x)Al_2O_3$ specimens is shown in Fig. 1. The h of specimens sintered at 1,450 °C increased firstly from 93.6% (x = 2.5) to 98.0% (x = 7.5) and then decreased to 93.4% (x = 15.0). Meanwhile, the h of specimens sintered at 1,500 °C exhibited slightly higher relative density with the same variation trend and reached the maximum of 98.8% for x = 7.5. It indicated that the sintering temperatures of $x La_2O_3/10Nb_2O_5$-$(90–x)Al_2O_3$ were 150~200 °C lower than that of Al_2O_3 ceramic (1,650 °C) [23]. The improvement of sinterability could be attributed to two reasons. On one hand, the doping of La_2O_3 and Nb_2O_5 might result in the formation of liquid phase during the sintering period. On the other hand, the volumetric heating enables microwave sintering to allow for more rapid and uniform heating than conventional sintering, leading to noticeable decreases in sintering temperature and time [24, 25].

The XRD patterns of the $x La_2O_3/10Nb_2O_5$-$(90–x)Al_2O_3$ ceramics are shown in Fig. 2. When x = 2.5, α-Al_2O_3 (ICDD: 46-1212) and $La_{0.33}NbO_3$ (ICDD: 53-1023) were detected. With the increase of the content of La_2O_3, $LaNbO_4$ (ICDD: 22-1125) and $LaAl_{11}O_{18}$ were formed successively. No diffraction peaks corresponding with La_2O_3 and Nb_2O_5 were observed. It indicated that $La_{0.33}NbO_3$, $LaNbO_4$ and $LaAl_{11}O_{18}$ were generated successively in the process of sintering when the mole ratio of La_2O_3 to Nb_2O_5 increased from 0.30:1 (x = 2.5) to 1.78:1 (x = 15.0). The phase compositions of $x La_2O_3/10Nb_2O_5$-$(90–x)Al_2O_3$ ceramics according to XRD analysis were listed in Table 1, which is similar to previous work from our group [26].

At the same time, when x exceeded 7.5, the intensities of diffraction peaks falling within $LaAl_{11}O_{18}$ increased, i.e., the content of $LaAl_{11}O_{18}$ ascended with the increasing La_2O_3 content. Of course, since La_2O_3 reacts with Al_2O_3, the content of Al_2O_3 is continuously decreasing. When x = 15.0, the main phase transformed from Al_2O_3 to $LaAl_{11}O_{18}$.

Fig. 3 is a presentation of the SEM images of $x La_2O_3/10Nb_2O_5$-$(90–x)Al_2O_3$ ceramics. All the specimens exhibited a very small number of pores because the high heating rate in microwave sintering is favorable to boundary diffusion and in turn grain growth [27, 28]. When x = 2.5, the specimen was consisted of equiaxed grains and fewer grain boundary phase, which were determined to be Al_2O_3 and $La_{0.33}NbO_3$, respectively, by the EDS analysis (as shown in Fig. 3(a)). $LaNbO_4$ grains were observed as x exceeded 2.5(as shown in Fig. 3(b)) and the amount of which increased with increasing x. Meanwhile, the Al_2O_3 grains for x > 2.5 were smaller than that for x = 2.5 and homogeneously distributed with $LaNbO_4$. As to x = 15.0, a large quantity of plate-like grains identified as $LaAl_{11}O_{18}$ were formed (as shown in Fig. 3(f)), indicating that there were $LaNbO_4$ and plate-like $LaAl_{11}O_{18}$ obtained in-situ during the sintering process. This phenomenon resembles what was previously reported by Brito et al. [14] and Zhang et al. [15]. As Fig. 2 demonstrates, the SEM and EDS analysis exhibited the results consistent with those of XRD analysis above.

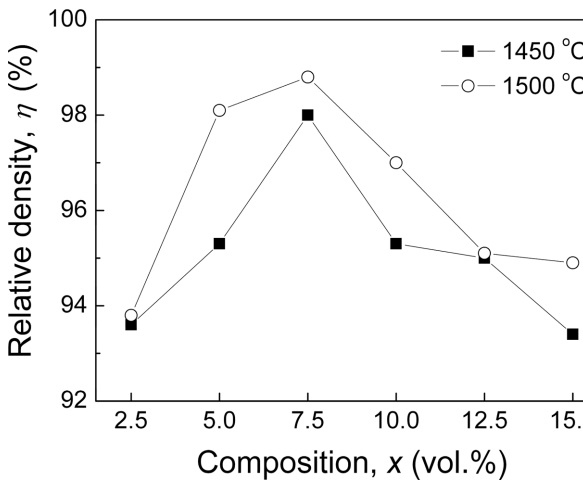

Fig. 1. Relative density (h) of $x La_2O_3/10Nb_2O_5$-$(90–x)Al_2O_3$ ceramics.

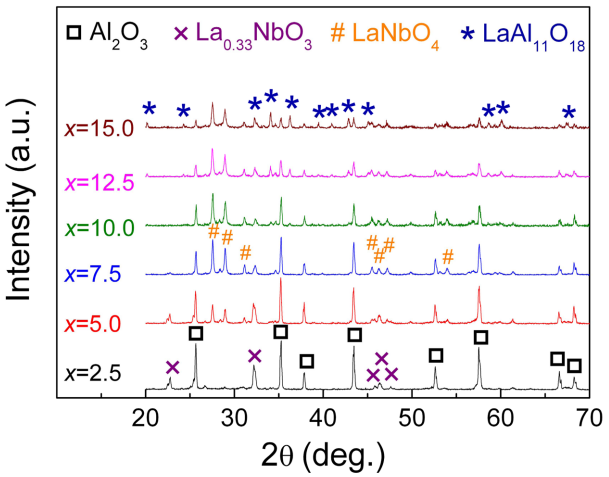

Fig. 2. XRD patterns of $x La_2O_3/10Nb_2O_5$-$(90–x)Al_2O_3$ ceramics.

Table 1. Phase composition of $x La_2O_3/10Nb_2O_5$-$(90–x)Al_2O_3$ ceramics.

x	Al_2O_3 ICDD: 46-1212	$La_{0.33}NbO_3$ ICDD: 53-1023	$LaNbO_4$ ICDD: 22-1125	$LaAl_{11}O_{18}$ ICDD: 33-0699
2.5	√	√		
5.0	√	√	√	
7.5	√		√	
10.0	√		√	√
12.5	√		√	√
15.0	√		√	√

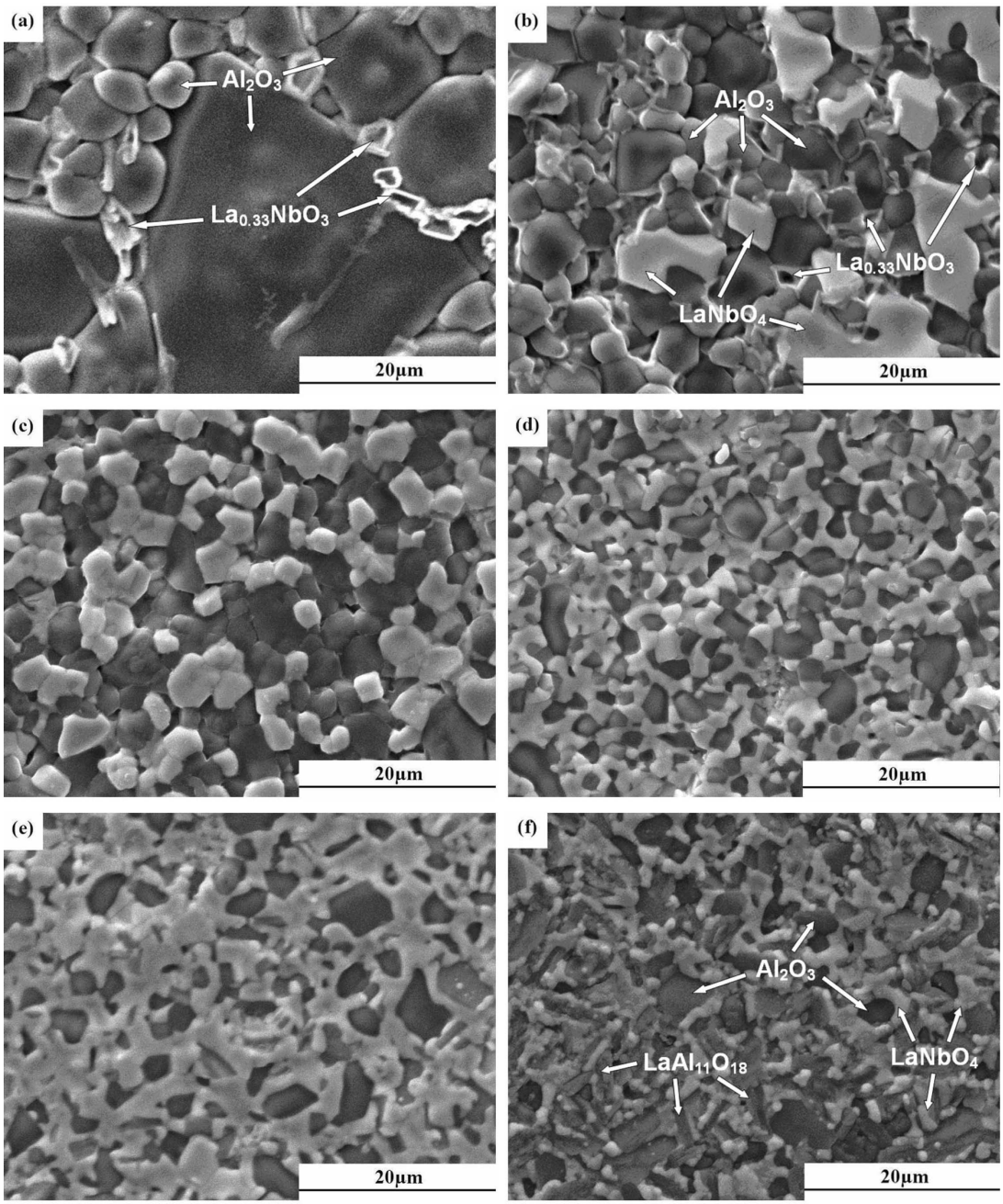

Fig. 3. SEM images of $x La_2O_3/10Nb_2O_5$-$(90–x)Al_2O_3$ ceramics sintered at 1,500 ºC for 30 min: (a)~(f), $x = 2.5$, 5.0, 7.5, 10.0, 12.5, 15.0, respectively.

The Vickers hardness (*Hv*) of $5Nb_2O_5/xLa_2O_3$-$(95–x)Al_2O_3$ composite ceramics was summarized in Fig. 4. As $2.5 \le x \le 15.0$, *Hv* of the specimens sintered at 1,500 ºC was higher, to some extent, than *Hv* of which sintered at 1,450 ºC. With the increase of *x* value, *Hv* increased firstly ($2.5 \le x \le 7.5$) and then decreased gradually ($7.5 \le x \le 15.0$), and it reached the maximum value for $x = 7.5$. All the samples exhibited *Hv* higher than 10.1 GPa. The highest value of *Hv* is 12.6 GPa ($x = 7.5$). The variation trend of *Hv* was similar to that of the relative density. As shown in Fig. 1, the specimens sintered at 1,500 ºC were denser than which sintered at 1,450 ºC. Therefore, when composition was determined, *Hv* of the former was higher than that of the latter [29].

Like Vickers hardness, as shown in Fig. 5, the fracture toughness (K_{IC}) of $xLa_2O_3/10Nb_2O_5$-$(90–x)Al_2O_3$ composite ceramics climbed to the maximum for $x = 7.5$ and then declined gradually with the increasing *x*. When $5.0 \le x \le 12.5$, the $xLa_2O_3/10Nb_2O_5$-$(90–x)Al_2O_3$ composite ceramics exhibited fracture toughness exceeding 5.3 $MPa \cdot m^{1/2}$, over 70% higher than that of Al_2O_3 ceramic (~3.0 $MPa \cdot m^{1/2}$) [2].

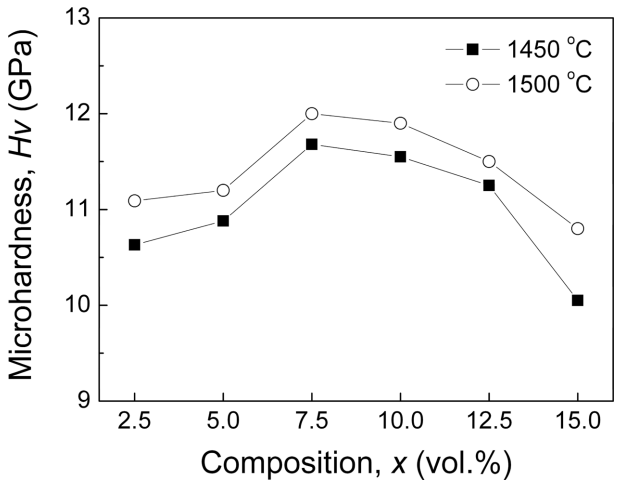

Fig. 4. Vickers hardness (*Hv*) of $x La_2O_3/10Nb_2O_5$-$(90–x)Al_2O_3$ ceramics.

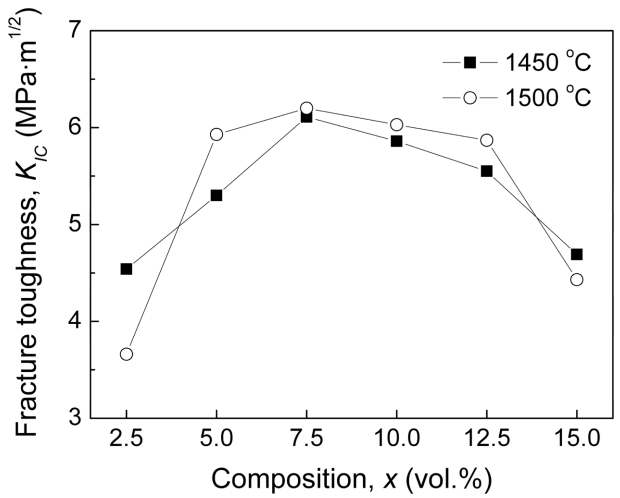

Fig. 5. Fracture toughness (K_{IC}) of $x La_2O_3/10Nb_2O_5$-$(90–x)Al_2O_3$ ceramics.

The micrographs of cracks propagation of $x La_2O_3/10Nb_2O_5$-$(90–x)Al_2O_3$ ($x = 7.5$) ceramics, originating from the corners of Vickers indentations, are presented in Fig. 6. $LaNbO_4$ grains reveal transgranular fracture and absorb energy through domain switch before cracking [28]. This sort of energy absorption performed by $LaNbO_4$ grains in $x La_2O_3/10Nb_2O_5$-$(90–x)Al_2O_3$ ceramics, in some extent, is similar to ZrO_2 in Al_2O_3 ceramics [10, 30]. Remarkably, few columnar Al_2O_3 grains (marked as C-A with arrows in Fig. 6) with length-diameter ratio of about 3:1 were formed, i.e., some Al_2O_3 grains were induced to grow oriented by the combined addition of La_2O_3 and Nb_2O_5. The existence of columnar Al_2O_3 grains in the path of crack propagation forced the cracks to deflect and diverge, extending the length of cracks. In general, the combined effects of domain switching of $LaNbO_4$, crack bridging and crack deflection play an important role in the significant improvement of the fracture toughness of

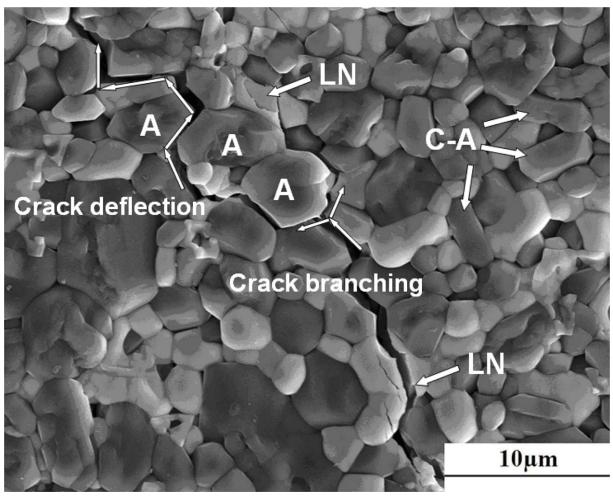

Fig. 6. SEM image of the crack propagation paths in $x La_2O_3/10Nb_2O_5$ -$(90–x)Al_2O_3$ ceramics(A: Al_2O_3, LN: $LaNbO_4$, C-A: Columnar Al_2O_3): $x = 7.5$, 1,500 °C, 30 min.

$x La_2O_3/10Nb_2O_5$-$(90–x)Al_2O_3$ ceramics. As a result, $7.5La_2O_3/10Nb_2O_5$-$82.5Al_2O_3$ ceramic exhibited high fracture toughness: 6.2 MPa·m$^{1/2}$(1,500 °C, 30 min).

Conclusions

$x La_2O_3/10Nb_2O_5$-$(90–x)Al_2O_3$ ceramics were synthesized via microwave sintering at 1,450~1,500 °C for 30 min. The relative densities of $x La_2O_3/10Nb_2O_5$-$(90–x)Al_2O_3$ ceramics are higher than 93%. The sintering temperature for preparing the composite ceramic was 150~200 °C lower than that of Al_2O_3 ceramic. $LaNbO_4$, columnar-Al_2O_3 grains and $LaAl_{11}O_{18}$ with plate-like shape were generated in-situ during the sintering period. The fracture toughness of $x La_2O_3/10Nb_2O_5$-$(90–x)Al_2O_3$ ceramics were enhanced by the synergistic effect of columnar-Al_2O_3 grains and domain-switched $LaNbO_4$ grains. Compared to Al_2O_3 ceramic, the fracture toughness of $x La_2O_3/10Nb_2O_5$-$(90–x)Al_2O_3$ ceramics were at least 70% higher when $5.0 \le x \le 12.5$. The $7.5La_2O_3/10Nb_2O_5$-$82.5Al_2O_3$ ceramic exhibited superior mechanical property: $Hv = 12.0$ GPa, $K_{IC} = 6.2$ MPa·m$^{1/2}$(1,500 °C, 30 min).

Acknowledgements

The authors gratefully acknowledge the financial support of the National Natural Science Foundation of China (No.51664043, No. 51802140 and No.51064022) and Natural Science Foundation of Jiangxi Province (20192BAB206007)

References

1. Q.B. Tian, J.S. Dai, Z.J. Lv, and T.G. Zhai, J. Ceram. Process. Res. 17[7] (2016) 676-680.
2. R. Danzer, T. Lube, P. Supancic, and R. Damani, Adv. Eng.

Mater. 10[4] (2008) 275-298.
3. J.K. Yoon and I.J. Shon, J. Ceram. Process. Res. 17[8] (2016) 876-880.
4. W. Acchar, C.A. Cairo, and A.M. Segadães, Mater. Sci. Eng. A 406[1-2] (2005) 74-77.
5. Z.B. Yin, C.Z. Huang, B. Zou, H.L. Liu, H.T. Zhu, and J. Wang, Mater. Sci. Eng. A 577 (2013) 9-15.
6. E.M. Sharifi, F. Karimzadeh, and M.H. Enayati, J. Alloys Compd. 491[1-2] (2010) 411-415.
7. M. Parchovianský, D. Galusek, J. Sedláček, P. Švančárek, M. Kašiarová, J. Dusza, and P. Šajgalík, J. Eur. Ceram. Soc. 33[12] (2013) 2291-2298.
8. S.C. Jeong, S.H. Ahn, and K.W. Nam, J. Ceram. Process. Res. 17[10] (2016) 1088-1094.
9. N.A. Rejab, A.Z.A. Azhar, M.M. Ratnam, and Z.A. Ahmad, Int. J. Refract. Met. Hard Mater. 36 (2013) 162-166.
10. V. Naglieri, P. Palmero, L. Montanaro, and J. Chevalier, Materials 6[5] (2013) 2090-2102.
11. Y.L. Ai, F. He, B.L. Liang, W. He, and W.H. Chen, Adv. Mater. Res. 338 (2011) 120-123.
12. Y.F. Hsu, Mater. Sci. Eng. A 399[1-2] (2005) 232-237.
13. Y.L. Ai, F. He, B.L. Liang, W. He, and W.H. Chen, Key Eng. Mater. 519 (2012) 265-268.
14. Y.Q. Wu, Y.F. Zhang, X.X. Huang, B.S. Li, and J.K. Guo, J. Mater. Sci. 36[17] (2001) 4195-4199.
15. Z.L. Zhang, L. Zhou, Y.G. Hu, and L. Jiang, Scripta Mater. 47[9] (2002) 637-641.
16. T. Takagi, Y.H. Choa, T. Sekino, and K. Nihara, Key Eng. Mater. 161-163 (1998) 181-184.
17. D.L. Johnson, Ceram. Int. 17[5] (1991) 295-300.
18. J.D. Katz, Annu. Rev. Mater. Sci. 22[1] (1992) 153-170.
19. A. Chatterjee, T. Basak, and K.G. Ayappa, AIChE J. 44[10] (1998) 2302-2311.
20. W. Liu, F. Xu, Y. Li, X. Hu, B. Dong, and Y. Xiao, Materials 9[3] (2016) 120.
21. K.H. Brosnan, G.L. Messing, and D.K. Agrawal, J. Am. Ceram. Soc. 86[8] (2003) 1307-1312.
22. Y. Bykov, S. Egorov, A. Eremeev, V. Kholoptsev, I. Plotnikov, K. Rybakov, and A. Sorokin, Materials 9[8] (2016) 684.
23. J.P. Cheng, D. Agrawal, Y.J. Zhang, and R. Roy, Mater. Lett. 56[4] (2002) 587-592.
24. C.Y. Fang, C.P. Wang, A.V. Polotai, D.K. Agrawal, and M.T. Lanagan, Mater. Lett. 62[17-18] (2008) 2551-2553.
25. H.S. Hao, L.H. Xu, Y. Huang, X.M. Zhang, and Z. P. Xie, Sci. China Ser. E 52[9] (2009) 2727-2731.
26. W. He, Y.L. Ai, B.L. Liang, W.H. Chen, and C.H. Liu, Mater. Sci. Eng. A 723 (2018) 134-140.
27. D. Zymelka, S. Saunier, D. Goeuriot, and J. Molimard, Ceram. Int. 39[3] (2013) 3269-3277.
28. Y. Liu, F.F. Min, J. B. Zhu, and M.X. Zhang, Mater. Sci. Eng. A 546 (2012) 328-331.
29. P. Figiel, M. Rozmus, and B. Smuk, J. Achi. Mater. Manu. Eng. 48[1] (2011) 29-34.
30. S. Abbas, S. Maleksaeedi, E. Kolos, and A. Ruys, Materials 8[7] (2015) 4344-4362.